Int J Energy Environ Eng (2017) 8:293–301
https://doi.org/10.1007/s40095-017-0247-3

ORIGINAL RESEARCH

Design of an airborne vertical axis wind turbine for low electrical power demands

Firman Bagja Juangsa[1] · Bentang Arief Budiman[2,3] · Muhammad Aziz[4] · Tubagus Ahmad Fauzi Soelaiman[2]

Received: 17 November 2016 / Accepted: 23 September 2017 / Published online: 4 October 2017

Abstract An airborne vertical axis wind turbine (VAWT) is a new approach in wind turbine development. In this paper, a new design of the airborne VAWT which can produce electricity for a light-emitting diode (LED) system is exhibited. A gas balloon is used as the turbine and features a special blade design to convert wind energy into rotation of the electrical generator. The turbine was designed to meet the characteristics of wind in limited terrestrial wind speed areas. The generator was designed to be lightweight whilst retaining favorable performance for electricity generation. Performance test results showed that the developed generator could provide the required power supply for a LED system. Moreover, the generator can also recharge the batteries used as a voltage regulator for the LED system.

Keywords Airborne wind turbines · Vertical axis wind turbines · Electrical generator · Gas balloon

✉ Bentang Arief Budiman
bentang@ftmd.itb.ac.id

[1] Department of Mechanical Sciences and Engineering, Tokyo Institute of Technology, Tokyo, Japan

[2] Faculty of Mechanical and Aerospace Engineering, Institut Teknologi Bandung, Ganesha Street No. 10, Bandung 40132, Indonesia

[3] National Center for Sustainable Transportation Technology, Institut Teknologi Bandung, Bandung, Indonesia

[4] Institute of Innovative Research, Tokyo Institute of Technology, Tokyo, Japan

Introduction

Wind has an excellent potential as an energy source because of its cleanliness, renewability, and wide availability [1, 2]. For many types of wind turbine, the main subsystems required to convert wind energy to electrical power have been developed [3, 4]. Currently, wind energy harvesting is focused on terrestrial wind, which is strongly influenced by relief, ground thermic, and coverage type [5]. Less attention has been paid to high-altitude wind, which is less influenced by these factors, leading to steadier, more persistent, and higher velocity wind energy. Generally, wind energy increases with altitude, leading to the idea of an altitude wind energy system [6–9].

To harvest high-altitude wind, the airborne wind turbine [10, 11] is considered to be an alternative and innovative method which has several advantages [12]. It can be operated at high altitude to capture wind energy without a tower. Higher altitudes experience increased wind speeds [13]; there are fewer obstacles for the wind, especially in cities that have many buildings. The absence of a tower also can reduce the production cost of the wind turbine by more than 10% [14]. Moreover, airborne wind turbines have an advantage in deployment flexibility. This is important for remote areas that have limited access to the grid, or for archipelagic countries that have many distributed islands, causing difficulties in grid access.

Energy harvesting of high-altitude wind is not a simple task, because of technical and policy difficulties [15]. Various methods to harvest high-altitude wind have been proposed, including ladder mill [16], pumping mill [17], tethered rotorcraft [18], and dirigible-based rotor [11]. In general, airborne wind turbines can be divided into two groups based on their rotation axis: vertical axis wind turbine (VAWT) and horizontal axis wind turbine (HAWT)

[19, 20]. An example of an airborne wind turbine with a horizontal axis was developed by Magenn air rotor system (MARS) [21]. Its design allows the turbine to be automatically oriented to capture the wind. Air rotors can be raised to an altitude of roughly 300 m. While the airborne HAWT is well established, there has been limited attention to the development of an airborne VAWT. This is because the VAWT generates relatively lower electrical power than the HAWT. Moreover, the design of a device that can operate about the vertical axis is challenging. However, the airborne VAWT has important advantages, especially for Savonius concept that has the ability to self-start and operate in low wind speed conditions [22]. Furthermore, the airborne VAWT has the ability to capture the wind from any direction because of its vertically positioned blades.

An innovative design of airborne VAWT is proposed and analyzed in this paper. The analysis focuses on the design of an airborne VAWT that can harvest the low-speed wind energy which characterizes tropical areas. The designed and manufactured airborne VAWT was evaluated to supply electrical power for a low-power 100 LED lights, i.e., 0.4 W. These LED lights can be utilized for many purposes including aircraft warning lights on tall buildings, advertising media, additional lighting for parking areas, and power supply for traffic lights. Drag-type blades were used to produce high torque at low wind speeds. The main design requirements were as follows: (1) the airborne wind turbine must be suitable for low wind speeds, (2) it has to work in any wind direction without yaw movement, and (3) it has to be stable in the vertical position during the operation to harvest wind energy at highest efficiency. In addition, several important parameters affecting airborne VAWT performance were calculated. A lightweight generator was also manufactured and tested according to the requirements of the LED illumination system.

The proposed design of airborne VAWT

The basic design of the proposed airborne VAWT was from a Savonius wind turbine, which is able to self-start and operate in low wind speed conditions [23]. A gas balloon was used as the main body of the turbine. Ideally, the airborne VAWT must be positioned vertically to operate in any wind direction. However, the swing movement of the gas balloon due to total drag force generated by wind (F_W) might occur, which reduces the harvested wind energy. This problem is a main challenging issue in designing the airborne VAWT. The problem can be solved by increasing the gas volume at the top of the balloon (head) as shown in Fig. 1a. Figure 1b shows free body diagram of the airborne VAWT without head component.

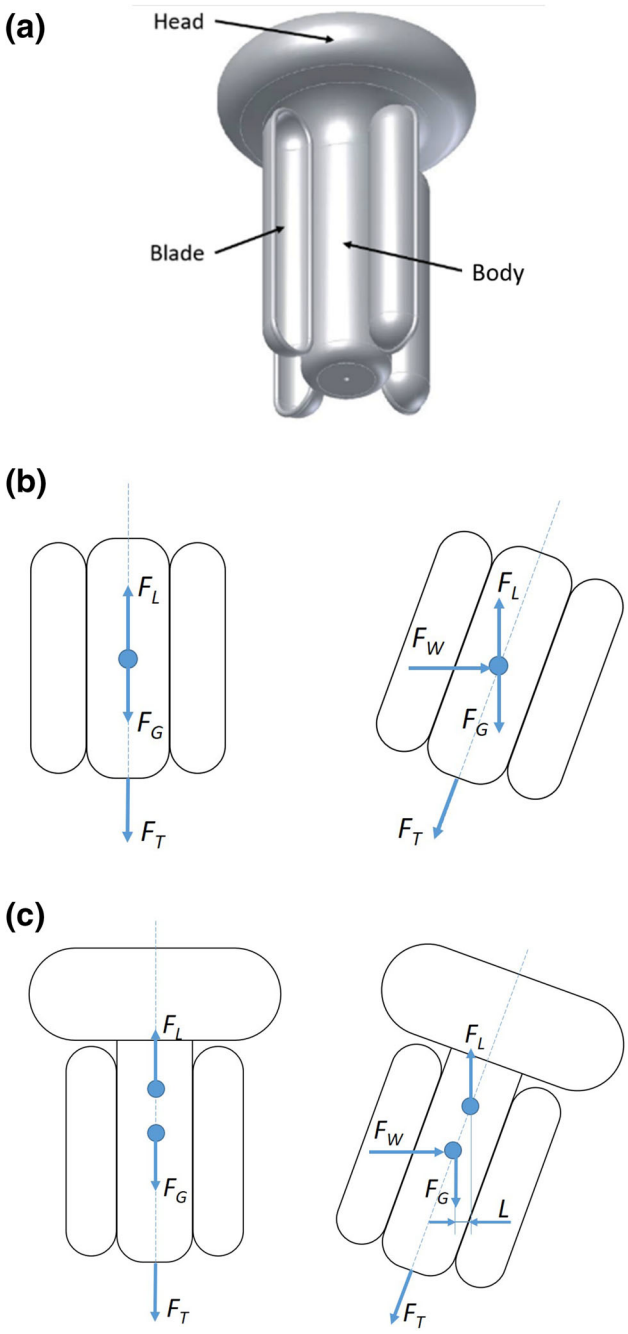

Fig. 1 **a** The proposed design of the airborne VAWT, **b** free body diagram without head component, and **c** with head component

In this case, F_W, gravitational force (F_G), lift force (F_L), and tie force (F_T) are coincident in the center of gravity point. Thus, the turbine is tilted following the swing movement. Figure 1c shows the airborne VAWT with head component. It is clearly seen that the position of total F_L is shifted from the center of gravity point due to the additional F_L in head component. This shifting can generate moment force ($F_L \times L$) if the turbine is tilted. Thus, the turbine has an automatic mechanism to maintain its vertical

position during the operation. Furthermore, the drag coefficient of the designed gas balloon head must be much lower than the blades, which will also increase the turbine stability.

The selection of the blade shape was also part of the proposed design; the half-round shape was selected to obtain the highest drag force [24]. The blade shape was selected to maximize the drag force, and convert the wind's transverse velocity into the rotational velocity of the turbine. Several important parameters including the number of the blades, the torque generated on each blade, and the operating rotational velocity were theoretically calculated.

Methodology

Number of blades

The number of blades used for the airborne wind turbine must be determined to obtain a maximum drag force [25]. Typically, increasing the number of blades installed to the VAWT can achieve high drag force from any direction of the wind [26]. However, there must be no blade which is covered by another blade whilst facing the wind. Figure 2a shows a schematic of the blade positions for the gas balloon. A covered blade is defined as when the outer part of a blade (point A) overlaps the tangential line of the inner part of another blade. The number of blades, while maintaining that there is no blade covered by another blade, reaches a maximum when point A is in line with the tangential line. At a maximum number of blades (n), point OAC will form a right triangle as shown in Fig. 2b. n can be then calculated from Eq. (1):

$$n = \frac{2\pi}{\theta}, \tag{1}$$

where θ is the angle of the nearest two blades. It can be calculated using the following equations:

$$\cos\theta = \frac{D/2}{D/2 + d}, \tag{2}$$

where D and d are the outer diameter of the gas balloon and the diameter of the blade, respectively. Substituting Eq. (2) into Eq. (1), n as a function of diameter ratio (D/d) can be calculated using Eq. (3):

$$n = \frac{2\pi}{\cos^{-1}\left(\frac{D/d}{D/d+2}\right)}. \tag{3}$$

Note that n is an integer number, the decimal number appearing from calculations should be rounded down.

Generated torque on the blades

The total torque generated by the blades (T) is generated when the blades are facing the wind. Hence, it can be calculated using Eq. (4):

$$T = \sum F_{\mathrm{D}} R \tag{4}$$

where R is the length between the center of the main gas balloon and the center of blade and F_{D} is the drag force generated by the blade. F_{D} in stationary condition can be calculated using Eq. (5):

$$F_{\mathrm{D}} = \frac{1}{2} C_{\mathrm{D}} \times \rho \times A \times (v\cos(\alpha))^2, \tag{5}$$

where ρ, A, v, α, and C_{D} are air density, the frontal area of the blade, wind speed, the angle between the wind speed direction and the normal direction of the blade surface, and drag coefficient, respectively. It is important to note that the blades of an airborne VAWT consist of front and back shapes. The value of C_{D} depends on the blade shape facing the wind. Forward torque is generated by the front shape of the blades facing the wind, whereas an opposing torque is generated by the back shape of the blades facing the wind.

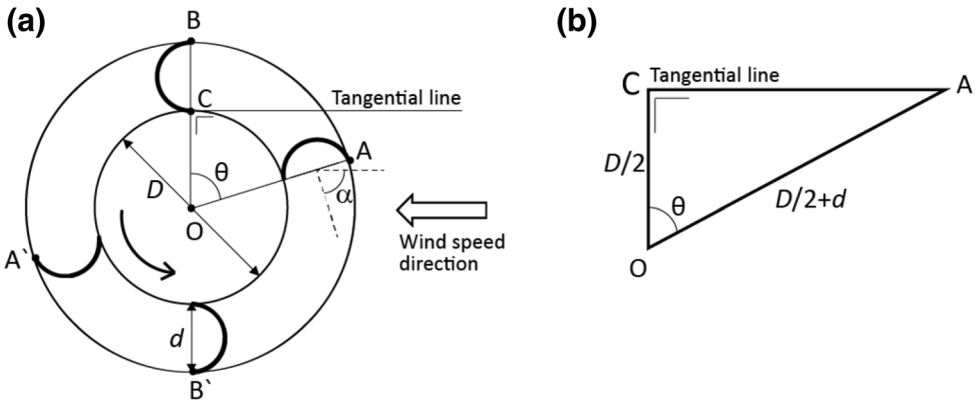

Fig. 2 **a** Schematic of blade position, **b** a right triangle used to calculate the maximum blade number condition

The total torque generated by the blades in stationary condition (T_{sta}) can be calculated using Eq. (6):

$$T_{sta} = \frac{1}{2}\rho \times A \times R \left(\sum_{1}^{i=m} C_{D1} \times (v\cos(\alpha_i))^2 - \sum_{1}^{j=n} C_{D2} \times (v\cos(\alpha_j))^2 \right), \quad (6)$$

where C_{D1} and C_{D2} are the drag coefficients of the front and back blade surfaces, respectively. m and n indicate a number of the front shape blades and back shape blades facing the wind, respectively.

Operating rotational velocity

The operating rotational velocity of an airborne VAWT (ω) can be predicted by modifying Eq. (6) for steady-state rotation. In steady-state rotation, the available wind speed which can generate a torque at the blade (T_{cycle}) is the relative speed between the wind speed and the circumferential speed of blade. F_D generated from the available wind is used to maintain the rotation of the airborne VAWT. Further, T_{cycle} can be expressed by Eq. (7):

$$T_{cycle} = \frac{1}{2}\rho \times A \times R \times \left(\sum_{1}^{i=m} C_{D1} \times (v\cos(\alpha_i) - \omega \times R)^2 - \sum_{1}^{j=n} C_{D2} \times (v\cos(\alpha_j) + \omega \times R)^2 \right). \quad (7)$$

Evaluating the proposed design

An airborne VAWT model was designed by considering the important parameters shown in Eqs. (3), (6), and (7). The turbine size was firstly determined by considering the manufacturing constraints. The largest gas balloon volume which could be manufactured was 4 × 4 × 6 m^3. From this constraint, the diameter of the gas balloon head was selected as 4 m to give a maximum additional F_L for the turbine.

n and D/d were also determined by considering the manufacturability of the gas balloon. Figure 3 shows the relationship between n and D/d calculated using Eq. (3). It can be seen that higher D/d causes high n which can imply low T due to small A. However, large D has to be selected to maintain lift force of the gas balloon. The proper design of gas balloon must simultaneously consider lift force of gas balloon and F_D of blade generating ω. It can occur by selecting a proper D/d value.

In the proposed design, the total weight of the turbine was 150 N, whereas the expected lift force from the gas balloon was 230 N. Hydrogen gas was used in the gas balloon due to its relatively low cost. Considering those design requirements, D/d of 1.56 was selected to assure the

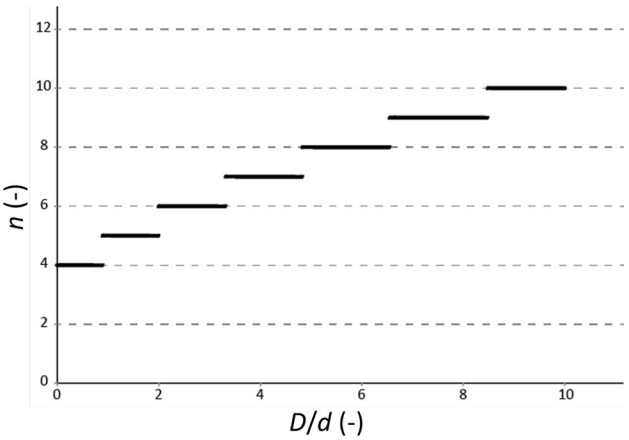

Fig. 3 Relation of maximum number of blades to ratio of diameter

condition for high T while maintaining the main body size (for lift force). From selected D/d, the possible maximum n is five blades.

To obtain a high T_{sta}, the difference in F_D between the front and back blades must be as large as possible. A half-round shape was selected for the blade, producing C_{D1} of 2.3 and C_{D2} of 1.1 [24]. T_{sta} calculations in Eq. (6) were conducted using parameters, such as ρ of 1.232 kg m^{-3}, v of 5 m s^{-1}, and A of 3.46 m^3. Figure 4 shows the results of the calculations which cover two configurations: four

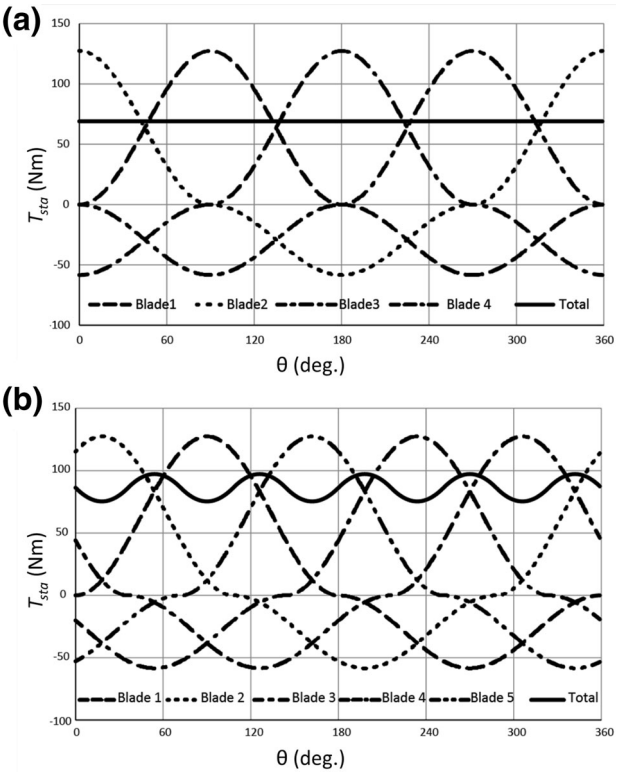

Fig. 4 Correlation of starting torque and blade position: **a** four blades, **b** five blades

blades (Fig. 4a) and five blades (Fig. 4b). It can be seen that T_{sta} generated by five blades is higher than four blades. However, T_{sta} curve is not constant in the five blades case. This phenomenon generally occurs if an odd number of blades are employed. The inconstant T_{sta} can cause tilt of gas balloon turbine or even the turbine collapse which drastically reduces the efficiency of conversion from wind speed to ω. A constant T_{sta} is important to ensure that the turbine rotates smoothly. Further, the constant T_{sta} technically simplifies the performance testing of generator designs. In a steady-state rotation, T_{cycle} generated was calculated using Eq. (7). The results for four and five blades are shown in Fig. 5a, b, respectively. The T_{cycle} generated by five blades is higher than four blades. However, by considering inconstant T_{sta} generated by five blades, four blades prefer to be selected for the turbine.

The airborne VAWT requires special generators design to convert wind energy to electric power for supplying the LED system [27]. In this study, a generator was designed to rotate and produce electricity at least for ω of 30 rpm. There are several parameters which can be modified in the design of a low-speed generator; these are shown in Table 1. For this work, the parameters were determined to generate sufficient power for 100 LED lights, while maintaining the lightweight generator design. Generator dimensions were determined by maximum weight

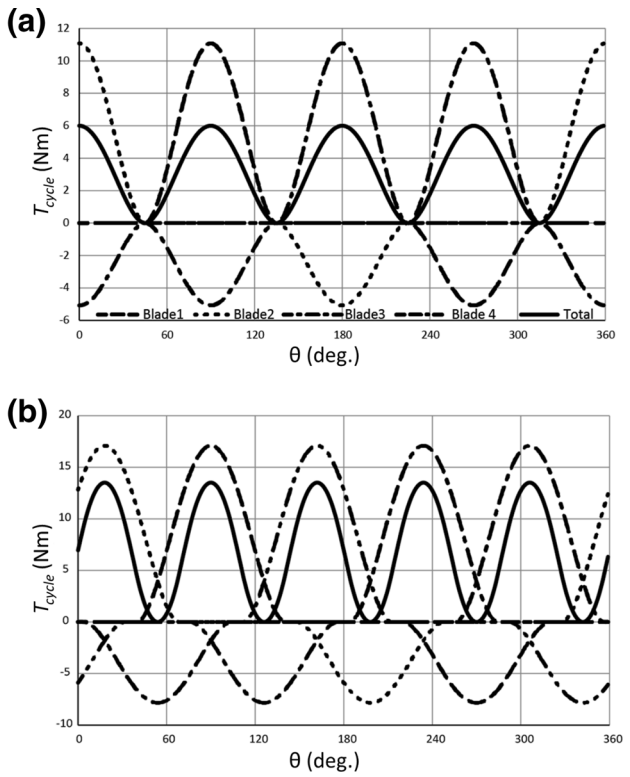

Fig. 5 Curves of steady-state rotation torque vs blade position: **a** four blades, **b** five blades

Table 1 Specifications of the generator

Parameter	Value
Diameter (m)	0.535
Number of magnets (pcs)	24
Number of winding (pcs)	12
Magnet dimension (mm^3)	0.03 × 0.012 × 0.005
Rotor dimension (m)	0.435
Magnetic field (T)	1.2
Electrical system (phase)	3
Winding formation (pcs $phase^{-1}$)	4 (serial)
Number of coils (coils)	400

limitation, while magnets were purchased with a predetermined specification. Finally, to fulfill the power requirement, the number of coils was determined based on the Faraday's law of electromagnetic induction.

An output voltage of generator generally depends on several factors including air gap, winding characteristic, flux flow, winding size, and winding configuration. The generator design was also constrained by the LED system; in this study, the generator is needed to power 100 LEDs. These LEDs were attached to the blades, and rotated with the gas balloon. The electrical system was equipped with a controller to manage the LED configuration: its illumination time and battery charging. The battery was utilized as power storage as well as a voltage regulator. The turbine charged the battery during the day and, in turn, the battery powered the LED system during the night. Lightweight nylon was selected as the material for the generator to ensure low weight. The generator had a winding formation; the number of winds was adjusted to achieve the lowest weight while maintaining a three-phase winding configuration. The details of generator winding and magnet configuration are shown in Fig. 6.

Experimental model and testing

The experimental model of airborne VAWT was created from a gas balloon made of polyvinyl chloride (PVC). The performance of the airborne VAWT model was then tested. It successfully rotated at 15–20 rpm under wind speeds 3–4 m s^{-1} at 800 m above sea level. It is noted that airborne VAWT was designed to rotate at 30 rpm under wind speed of 5 m s^{-1}.

The low-speed generator as a key component to generate electric power was manufactured using a computerized numerical control (CNC) milling process to ensure the roundness of both rotor and stator. Several slots were milled on the stator and the rotor to mount the magnets and the winding. These slots needed to be precise because they can

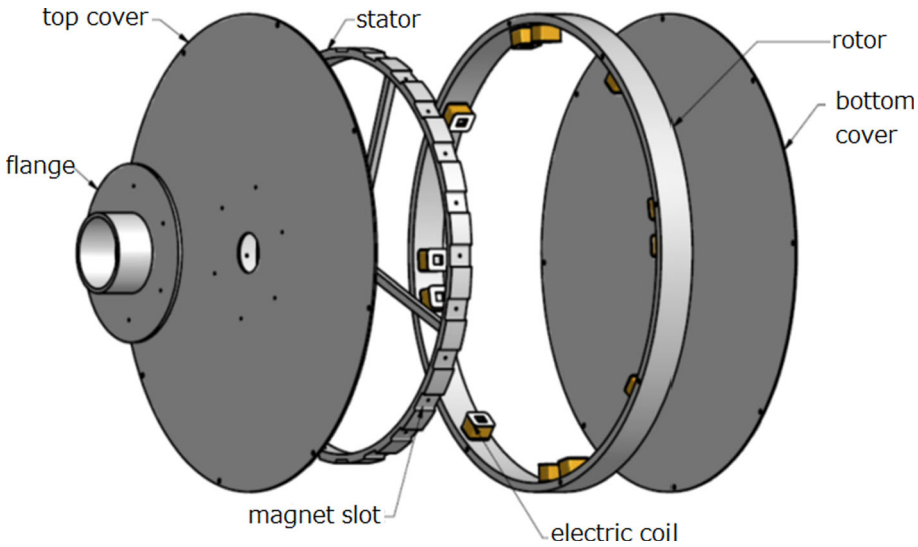

Fig. 6 Generator configuration

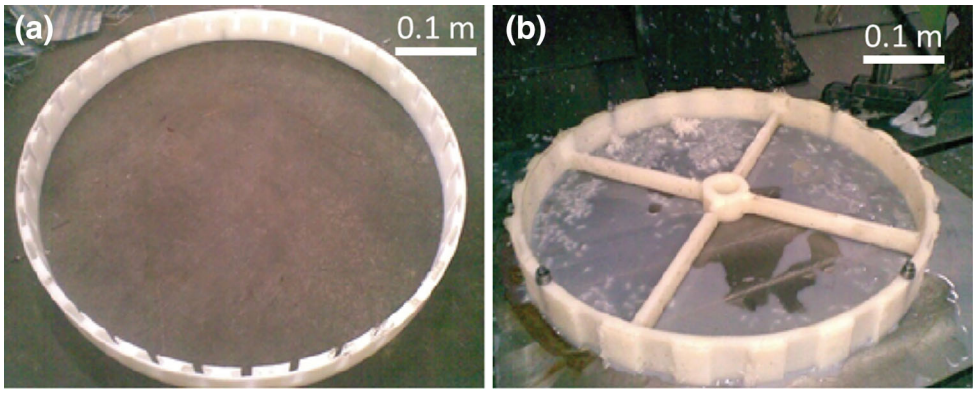

Fig. 7 Overview of the developed motor: **a** rotor, **b** stator

influence the output voltage of the generator. Figure 7a, b shows the manufactured rotor and stator, respectively.

The magnet was mounted on the stator using a bolted connection, whilst winding and core iron was mounted in the previously created slot on the rotor. The shaft system allows the rotor to rotate relative to the stator. It has two bearings that were mounted on the shaft and aluminum pipe placed within the balloon. The torque was transmitted by a flange from the turbine to the rotor of generator. So, the winding and core iron rotates together with the balloon and the electrical system.

The low-speed generator testing was conducted separately to measure its performance independently. Three tests of generator performance were conducted. The first test investigated the zero-load performance as shown in Fig. 8a. The generator was connected to an electric motor driver through a coupling. The ω of the electric motor can be controlled using an inverter, which allows the test using several values of ω. The AC electric power produced by the generator was converted to DC by a rectifier. Open circuit was firstly installed next to the rectifier in which the voltage generated by the generator was measured by voltmeter placed parallel to the circuit. The generator voltages for each ω were then measured as shown in Fig. 8b. It can be seen that the generator voltage could exceed the battery voltage of 4.5 V, which can turn on 100 LED lights properly. The voltage difference between generator and battery indicated that generator could deliver charging current to the battery, which means that the generator can charge the battery at ω of 30 rpm or more. Further, the linear relationship between the generator voltage and ω was also observed in the testing results.

The second test investigated the performance of the generator that charges the battery with the appropriate charging current. The battery was placed as a load that must be charged whereas no load from LED lights. This condition can occur at a day time. The investigation can be applied by setting closed circuit system next to the rectifier with Ampere meter placed series to the circuit as shown in Fig. 9a. Figure 9b shows the charging current to the battery

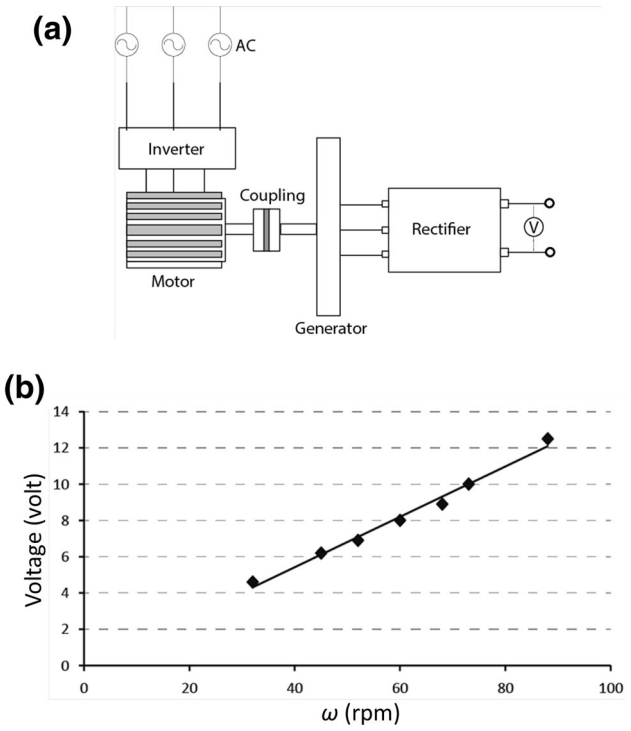

Fig. 8 **a** Schematic diagram of the low-speed generator testing with open circuit installed and **b** relationship between voltage and rotational velocity under no load condition

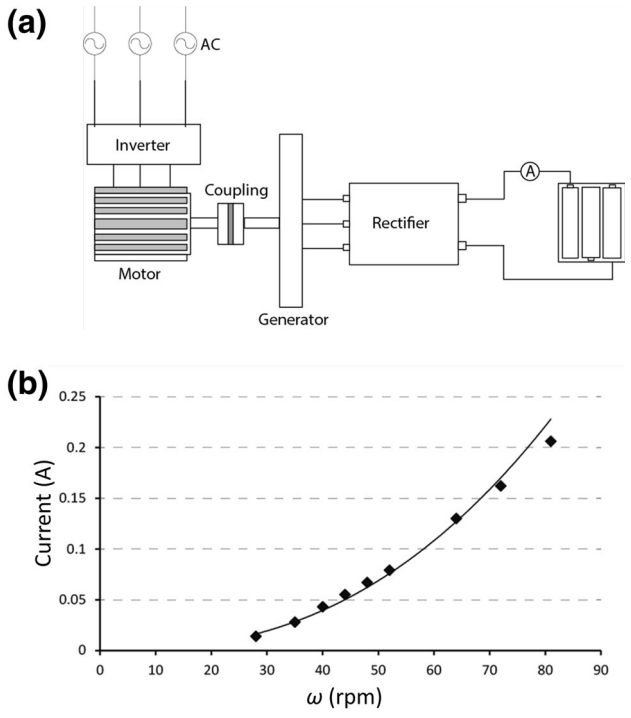

Fig. 9 **a** Schematic diagram of the low-speed generator testing with closed circuit installed and **b** relationship between current and rotational velocity during charging

measured using the Ampere meter. The charging time is mainly determined by the charging current. It is noted that the battery is difficult to be charged if the ω is less than 30 rpm due to the very low charging current.

The third test was conducted by measuring the overall generator performance, i.e., the generator was rotated by an electric motor at various ω. Batteries and LED system were represented by an adjustable potentiometer with a variable electrical resistor as shown in Fig. 10a. For each ω, the electrical resistor was adjusted from open circuit condition

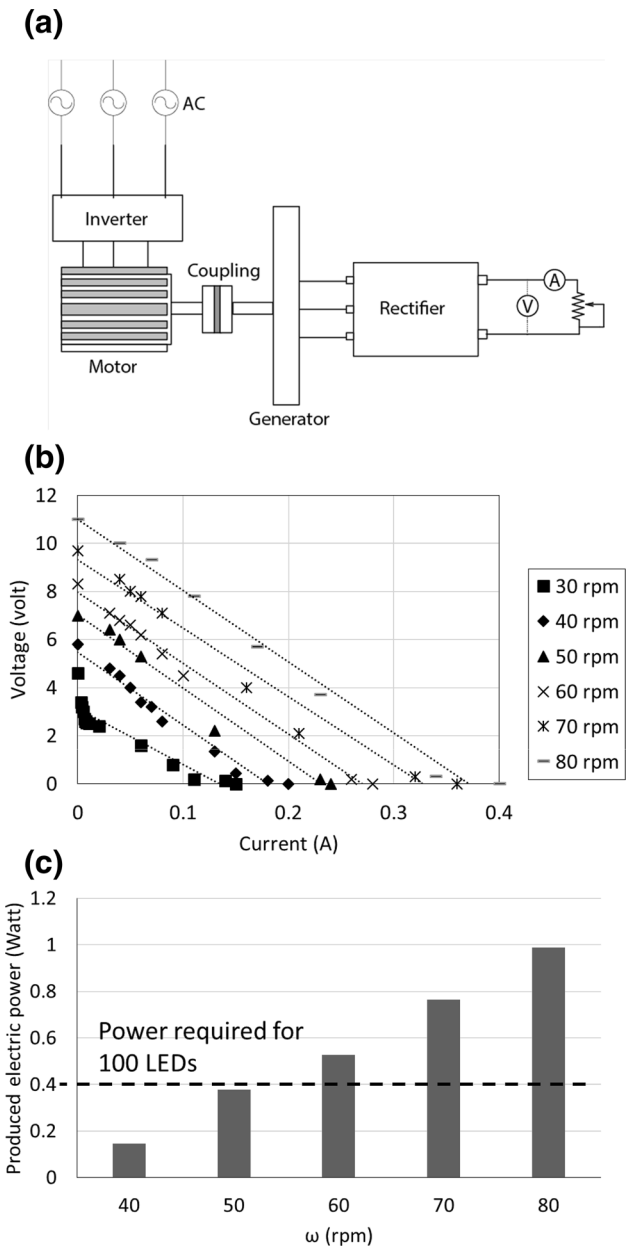

Fig. 10 **a** Schematic diagram of overall testing of generator performance, **b** voltage vs current relationship and **c** averaged electric power produced by generator at different angular velocities

(zero current) to short circuit condition (zero resistance). Figure 10b shows that the generator had favorable characteristics, as evidenced by the voltage–current curves at different rotational velocities. Electric power (voltage × current) produced by the generator at each ω can be determined from the battery voltage (4.5 V) multiplied by the measured electric current. The electric current value is determined based on a linear fitting line of *V–I* curves. From Fig. 10c, it is clearly seen that the 100 LED lights requiring 0.4 W can be fully supplied by the generator if ω is 60 rpm. This means, for ω less than 60 rpm, although the generator can still produce the electric power, it cannot fulfill overall required power for lightening the LED lights. For that reason, the battery as electric power source plays an important role in keeping turning on LED lights at the night. Further, the battery can be charged at the day time. In contrast, for ω of 60 rpm or more, the developed generator can fully supply the 100 LED lights and charge the battery simultaneously.

Conclusion

An airborne VAWT was designed for low electrical energy demands. Favorable performance was obtained during performance evaluation experiments. The problem in stabilizing the airborne VAWT was solved by introducing a special design, i.e., by increasing the gas volume in the top of the turbine (head). The turbine meets the design requirement for generating electrical power for lighting, i.e., the turbine rotates 30 rpm for wind speed of 5 m s^{-1}. A low-speed generator was designed and manufactured to produce electric power at least for the turbine rotating speed of 30 rpm. The evaluation of generator performance showed that it meets expectations, i.e., that it can generate electrical power for 100 LED lights and charge the battery. By designing an innovative airborne VAWT, utilization of low wind speeds for generating electric power, which is previously difficult, can be realized.

References

1. Kadiyala, A., Kommalapati, R., Huque, Z.: Characterization of the life cycle greenhouse gas emissions from wind electricity generation systems. Int. J. Energy Environ. Eng. **8**, 55–64 (2017)
2. Fazelpour, F., Tarashkar, N., Rosen, M.A.: Short-term wind speed forecasting using artificial neural networks for Tehran. Iran. Int. J. Energy Environ. Eng. **7**, 377–390 (2016)
3. Ghosh, A., Biswas, A., Sharma, K.K., Gupta, R.: Computational analysis of flow physics of a combined three bladed Darrieus Savonius wind rotor. J. Energy Inst. **88**, 425–437 (2015)
4. Ackermann, T., Söder, L.: Wind energy technology and current status: review. Renew. Sustain. Energy Rev. **4**, 315–374 (2000)
5. Bronstein, M.G.: Harnessing rivers of wind: a technology and policy assessment of high altitude wind power in the US. Technol. Forecast. Soc. **78**, 736–746 (2011)
6. Fagiano, L., Milanese, M.: Airborne wind energy: an overview. In: Proceedings of the 2012 American Control Conference, Montreal, Canada, pp. 3132–3143 (2012)
7. Ahrens, U., Diehl, M., Schmehl, R. (eds.): Airborne wind energy. Springer, Berlin (2013). ISBN 978-3642399640
8. Archer, C.L., Caldeira, K.: Global assessment of high-altitude wind power. Energies **2**, 307–319 (2009)
9. Archer, C.L., Delle Monache, L., Rife, D.L.: Airborne wind energy: optimal locations and variability. Renew. Energy **64**, 180–186 (2014)
10. Perkovic, L., Silva, P., Ban, M., Kranjcevic, N., Duic, N.: Harvesting high altitude wind energy for power production: the concept based on Magnus effect. Appl. Energy **101**, 151–160 (2013)
11. Magenn Power Inc. http://www.magenn.com/technology.php. Accessed Feb 2015)
12. Kolar, J.W., Friedli, T., Krismer, F., Looser, A., Schweizer, M., Friedemann, R.A., Steimer, P.K., Bevirt, J.B.: Conceptualization and multi-objective optimization of the electric system of an airborne wind turbine. IEEE Trans. Emerg. Sel. Top. Power Electron. **1**, 32–55 (2013)
13. Arya, S.: Introduction to Micrometeorology. Academic Press, New York (1988)
14. Fingersh, L., Hand, M., Laxson, A.: Wind turbine design cost and scaling model, NREL Technical Report, NREL/TP-500-40566, December 2006
15. Fagiano, L., Milanese, M., Piga, D.: High-altitude wind power generation. IEEE Trans. Energy Convers. **25**, 279–293 (2010)
16. Ockels, W.J.: Laddermill: a novel concept to exploit the energy in the airspace. Aircr. Des. **4**, 81–97 (2001)
17. Lansdorp, B., Ockels, W.J.: Comparison of concepts for high-altitude wind energy generation with ground based generator. In: Proceedings of 2nd China International Renewable Energy Equipment and Technology Exhibition and Conference, Beijing, China, pp. 1–9 (2005)
18. Roberts, B.W., Shepard, D.H., Caldeira, K., Cannon, M.E., Eccles, D.G., Grenier, A.J.: Harnessing high-altitude wind power. IEEE Trans. Energy Convers. **22**, 136–144 (2007)
19. Pope, K., Dincer, I., Naterer, G.F.: Energy and exergy efficiency comparison of horizontal and vertical axis wind turbines. Renew. Energy **35**, 2102–2113 (2010)
20. Schubel, P.J., Crossley, R.J.: Wind turbine blade design. Energies **5**, 3425–3449 (2012)
21. Ashwanth, Y.P., Ganesh, P.V., Arunprakash, E., Benisha, S.: Airborne power station (Mars the future wind-mill). IOSR J. Electr. Electron. Eng. **2**, 10–13 (2012)
22. Shamsoddin, S., Porté-Agel, F.: Large Eddy simulation of vertical axis wind turbine wakes. Energies **7**, 890–912 (2014)
23. Alaimo, A., Esposito, A., Milazzo, A., Orlando, C., Trentacosti, F.: Slotted blades Savonius wind turbine analysis by CFD. Energies **6**, 6335–6351 (2013)
24. Blevins, R.D.: Applied Fluid Dynamic Handbook. Krieger, Florida (2003)

25. Izadi, M., Bahrami, A., Aidun, D.K., Marzocca, P., Ghebreselassie, B., Williams, M.: Studying the effect of number of blades on the aerodynamic performance of a venturi effect fluid turbine (VEFT) by numerical simulation. In: The ASME 2011 International Mechanical Engineering Congress and Exposition (IMECE), vol. 6, pp. 1253–1262 (2011)
26. Wenehenubun, F., Saputra, A., Sutanto, H.: An experimental study on the performance of Savonius wind turbines related with the number of blades. Energy Proc. **68**, 297–304 (2015)
27. Duong, M.Q., Grimaccia, F., Leva, S., Mussetta, M., Sava, G., Costinas, S.: Performance analysis of grid-connected wind turbines. UPB Sci. Bull. Ser. C **76**, 169–180 (2014)